Quantifying the Influence of Specimen Geometry on the Results of the Restrained Ring Test

Moon, Jae-Heum; Rajabipour, Farshad; Pease, Bradley Justin; Weiss, Jason

Published in:
A S T M International. Journal

Publication date:
2006

Document Version
Publisher's PDF, also known as Version of record

Journal of ASTM International, Vol. 3, No. 8
Paper ID JAI100436
Available online at www.astm.org

Jae-Heum Moon,[1] *Farshad Rajabipour,*[2] *Brad Pease,*[3] *and Jason Weiss*[4]

Quantifying the Influence of Specimen Geometry on the Results of the Restrained Ring Test

ABSTRACT: Over the last decade, the restrained ring test has frequently been used to assess the cracking susceptibility of a concrete mixture when it is restrained from shrinking freely. Despite the frequent use of the ring test, limited analysis has been performed to understand how the specimen geometry influences the results of the test. This paper discusses the influence of specimen geometry on the results of the ring test considering three conditions: (1) uniform shrinkage of the concrete ring, (2) shrinkage caused by drying from the top and bottom surfaces of the concrete ring, and (3) shrinkage caused by drying from the outer circumference of the concrete ring. The role of moisture gradients, thickness of the concrete and the restraining (i.e., steel) rings, and the stiffness of concrete are considered in a series of numerical simulations. Results from these simulations can enable better selection of test specimen geometries and interpretation of the results from the ring test. Analytical expressions are provided to use for determining the geometry of the ring specimen that better simulates specific field conditions while providing the most useful information from the test.

KEYWORDS: autogenous shrinkage, concrete, cracking, degree of restraint, drying shrinkage, moisture gradient, shrinkage cracking, restrained ring test

Introduction

Cementitious materials change volume as a result of autogenous, drying, or thermal shrinkage. When these volume changes are prevented by the structure surrounding concrete, residual tensile stresses can develop inside the material. If these residual stresses exceed the tensile strength of concrete, cracking may occur. Over the years, engineers have sought to develop simple tests to assess how susceptible a given concrete mixture may be to shrinkage cracking. While tests like ASTM C 157-04 (Standard Test Method for Length Change of Hardened Hydraulic-Cement Mortar and Concrete) are frequently used to measure the free shrinkage of a concrete mixture, free shrinkage by itself is not sufficient to predict whether cracking will occur. Rather, the potential for cracking is dependent on the interaction of several factors, including the magnitude of free shrinkage, rate of shrinkage, elastic modulus, degree of restraint, creep/stress relaxation, and fracture toughness [1].

Several researchers have developed experimental procedures to study how material properties influence the potential for shrinkage cracking [2–4]. Several of these test procedures have been suggested to evaluate residual stresses that develop in concrete when shrinkage is restrained. Examples of such tests include the restrained ring test [5,6], the passive linear restraint tests [7,8], and the active linear restraint tests [9–11]. While a review of these test methods can be found elsewhere [12], this paper focuses on assessing the degree of restraint and the measurable strain in the restrained ring test.

Due to its simplicity and low cost, the restrained ring test has been used by numerous researchers to assess the potential for shrinkage cracking in concrete mixtures [3,5,12–14]. The ring test consists of a concrete annulus that is cast around a steel ring. As the concrete ring dries, it attempts to shrink. The steel ring prevents this shrinkage causing tensile stress to develop in the concrete. If these stresses are large enough, cracking may occur. Various geometries of the ring test have been used by researchers. AASHTO PP34-99 (AASHTO Standard Practice for Cracking Tendency Using a Ring Specimen) was developed as

Manuscript received June 8, 2005; accepted for publication July 11, 2006; published online August 2006.
[1] Ph.D. student, School of Civil Engineering, Purdue University, West Lafayette, IN 47907.
[2] Ph.D. student, School of Civil Engineering, Purdue University, West Lafayette, IN 47907.
[3] M.S.C.E. student, School of Civil Engineering, Purdue University, West Lafayette, IN 47907.
[4] Corresponding Author, Associate Professor, School of Civil Engineering, Purdue University, West Lafayette, IN 47907; e-mail: wjweiss@ecn.purdue.edu.

a provisional standard test method for assessing the cracking potential of a concrete mixture when it is restrained. AASHTO PP34-99 uses a 12.5-mm-thick steel ring, a 75-mm-thick concrete ring, and allows the concrete to dry from the outer circumference. While this method has been used in several studies, it has been reported that the low degree of restraint provided by the steel ring results in a fairly long time before the first visible cracking is observed [15]. As a result, an alternative test geometry was developed for inclusion as an ASTM standard (ASTM C 1581-04: Standard Test Method for Determining Age at Cracking and Induced Tensile Stress Characteristics of Mortar and Concrete Under Restrained Shrinkage). ASTM C 1581-04 uses a 12.5-mm-thick steel ring, however the concrete wall thickness was reduced to 37.5 mm to encourage cracking to develop at an earlier age. This restriction in specimen size, however, makes it difficult to test concrete with a larger aggregate or fiber reinforcement.

While the development of these standards is a positive step forward, it should be noted that the restrained ring test is not intended to measure a fundamental material property; rather, the ring test measures the material's response to a specific stimulus (e.g., drying at a constant temperature and relative humidity) under specific boundary conditions (e.g., specimen size, drying direction, and degree of restraint). No one specimen geometry or external stimulus can be used to simulate all the possible conditions that may be encountered in the field. It is therefore important that procedures are developed to enable the ring test to be interpreted for a variety of applications. Specifically, this may include applications where the degree of restraint provided by the structure may vary over a wide range (15–90 %) [16] or when the surface to volume ratio (this is analogous to varying thickness) of the concrete may vary from structure to structure. For example, the developer of a repair material may want to test their material under a high degree of restraint with a rapid rate of shrinkage to simulate a thin fully bonded repair. Alternatively, someone developing a bridge deck mixture may be more interested in testing a thicker section (i.e., slower overall shrinkage rate) with a lower degree of restraint.

This paper describes results of a study specifically looking at how various geometric factors influence the results of the ring test. An analytical solution is presented that describes the degree of restraint as a function of test geometry and material properties. Finite element simulations are performed to quantify how material properties, geometry, and drying direction influence the degree of restraint. It is intended that the results of these simulations will improve how the restrained ring test is used since it helps tailoring the ring geometry for specific applications.

Ring Specimen Geometry

Figure 1 shows the typical geometry of the restrained ring test. This paper will focus primarily on assessing two aspects of the restrained ring test: the influence of the drying direction and the influence of steel ring thickness.

First, the influence of the drying direction is considered. The simplest case which is encountered consists of uniform shrinkage throughout the concrete in both the radial and height directions. This may be observed in the cases of autogenous shrinkage and in many of the basic analytical modeling approximations. The second drying condition that is considered is drying from the top and bottom of the concrete ring. This geometry may be preferred compared to circumferential drying since it allows the concrete ring to be sufficiently thick to enable large aggregate and fiber reinforced concretes to be tested [17]. Top and bottom drying results in a uniform shrinkage along the radial direction but not along the height direction. Since both the uniform shrinkage and top and bottom drying conditions have uniform shrinkage along the radial direction, the residual stresses that develop in these cases are the highest at the inner radius of the concrete ring and decrease as a function of $1/r^2$ (where r is radial distance) through the concrete wall thickness [6]. The third drying condition considered in this paper is the case of circumferential drying as suggested by the standard testing procedures ASTM C 1581-04 and AASHTO PP34-99. In specimens that dry from the outer circumference, shrinkage is uniform through the height of the specimen but not through the radial direction. Since the specimen loses the majority of water at the circumference (i.e., drying face) the stresses are highest at the drying face [18–20]. This results in a complicated stress distribution which changes shape over time.

In addition to considering drying direction, this paper investigates the influence of steel ring thickness. A thicker steel ring will provide a higher degree of restraint, resulting in higher stress development in the concrete. On the other hand, the increase of the steel ring thickness decreases the magnitude of strain that

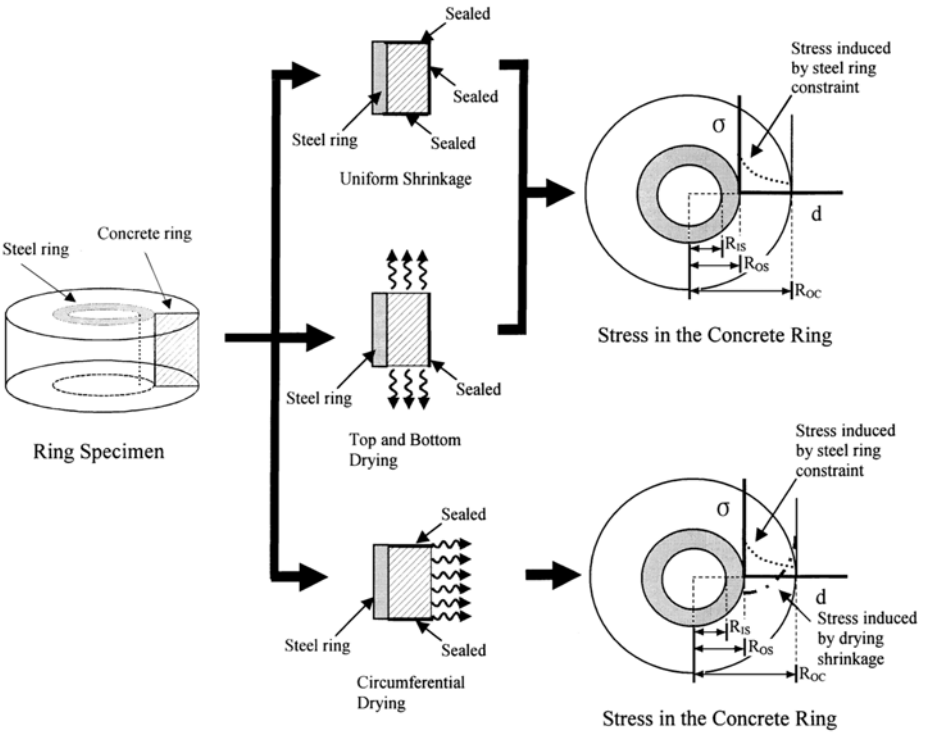

FIG. 1—*Drying direction and the resulting stress development of restrained ring.*

can be measured at the inner surface of the steel ring which is needed for stress calculations inside concrete [6]. Therefore, it is necessary to quantify how the thickness of the steel ring changes the degree of restraint as well as the stress measurements.

Quantifying the Degree of Restraint under Uniform Shrinkage (Analytical Approach)

Figure 2 can be used to provide a basic illustration of the concept of the degree of restraint [21]. In this conceptual example, a concrete prism is thought to be axially restrained by a steel prism (Fig. 2(*a*)). If the concrete shrinks and there is no connection between the concrete and steel (free boundary condition), a difference in length of specimens will exist as illustrated in Fig. 2(*b*). This difference is what one would expect to measure in a free shrinkage test like ASTM C 157-04. If the concrete is restrained by the steel prism (assuming bending is prevented), the concrete and steel will deform together (Fig. 2(*c*)). This will result in some of the shrinkage of the concrete being prevented resulting in a smaller length change than a specimen under free shrinkage condition. The degree of restraint (ψ) can be defined as:

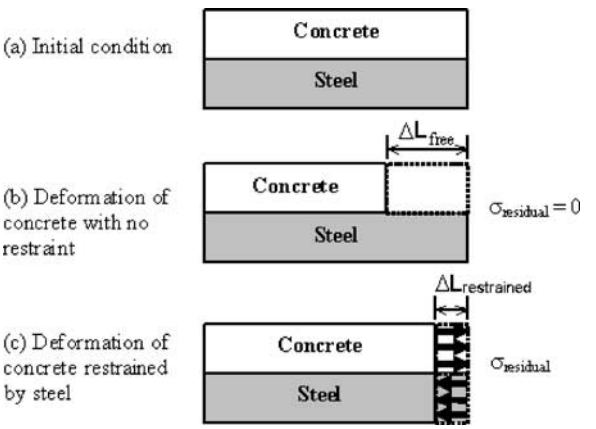

FIG. 2—*A conceptual illustration of the degree of restraint.*

$$\psi = \frac{\Delta L_{free} - \Delta L_{restrained}}{\Delta L_{free}} = 1 - \frac{\Delta L_{restrained}}{\Delta L_{free}} \tag{1a}$$

where ΔL_{free} is the displacement of concrete due to free shrinkage, and $\Delta L_{restrained}$ is the displacement of concrete under restraint as shown in Fig. 2. The degree of restraint can be estimated for linear specimens using Eq 1b [22]

$$\psi = \frac{E_C A_C}{E_C A_C + E_S A_S} \tag{1b}$$

where A_C and A_S are the cross-sectional areas, and E_C and E_S are the elastic moduli of concrete and steel elements, respectively. In the case of a restrained ring test, the degree of restraint can be written as Eq 1c:

$$\psi = \frac{U_{SH|R_{IC}}(t) - U_{S|R_{OS}}(t)}{U_{SH|R_{IC}}(t)} \tag{1c}$$

where $U_{SH|RIC}(t)$ is the free shrinkage displacement of the concrete ring (i.e., if no steel ring was present) measured at the inner surface of the concrete ring (R_{IC}) and $U_{S|Ros}(t)$ is the actual displacement of the concrete ring under the restraint provided by the steel ring. The degree of restraint in Eq 1c is defined at the concrete-steel interface (R_{IC}=R_{OS}; Fig. 1) where the restraint is maximum. The degree of restraint can vary between zero (corresponding to no restraint; $U_{SH|RIC}$=$U_{S|Ros}$) and one (corresponding to perfect restraint; $U_{S|Ros}$=0).

For the case of uniform shrinkage (i.e., no moisture gradient), the free shrinkage displacement, $U_{SH|RIC}(t)$ can be calculated using Eq 2a based on the linear free shrinkage of the concrete, $\varepsilon_{SH}(t)$ [12]:

$$U_{SH|R_{IC}}(t) = \varepsilon_{SH}(t) R_{IC} \tag{2a}$$

The actual displacement of the restrained concrete ring at R_{OS}, $U_{S|Ros}(t)$, can be calculated using the strain that is measured on the inner surface of the steel ring ($\varepsilon_{st}(t)$) as shown in Eq 2b.

$$U_{S|R_{OS}}(t) = \varepsilon_{st}(t) \frac{1}{2R_{OS}} [R_{OS}^2 + R_{IS}^2 - \nu_S (R_{OS}^2 - R_{IS}^2)] \tag{2b}$$

where ν_S is the Poisson's ratio of steel. By substituting 2a and 2b into 1c, the degree of restraint can be written as follows:

$$\psi = 1 - \frac{1}{2} \frac{\varepsilon_{st}(t)}{\varepsilon_{SH}(t)} \left[\frac{R_{IS}^2}{R_{OS}^2} (1 + \nu_S) + (1 - \nu_S) \right] \tag{3}$$

Meanwhile, the ratio $\varepsilon_{st}(t)/\varepsilon_{SH}(t)$ can be related to the specimen geometry and the material properties of concrete and steel by considering the interfacial pressure that develops at the concrete-steel interface. The magnitude of the interfacial pressure can be calculated using either Eq 4a, which is based on the measured steel strain from an experiment, or Eq 4b, which is based on fundamental computation made using a "shrink-fit" approximation that incorporates on the free shrinkage strain of the concrete and elastic properties of the concrete and steel [6,23]:

$$p_0 = -\varepsilon_{st}(t) E_S \frac{R_{OS}^2 - R_{IS}^2}{2R_{OS}^2} \tag{4a}$$

$$p_0 = -\frac{\varepsilon_{SH}(t) E_C'}{\frac{E_C'}{E_S} \frac{[(1+\nu_S)R_{IS}^2 + (1-\nu_S)R_{OS}^2]}{(R_{OS}^2 - R_{IS}^2)} + \frac{[(1-\nu_C)R_{OS}^2 + (1+\nu_C)R_{OC}^2]}{(R_{OC}^2 - R_{OS}^2)}} \tag{4b}$$

In these equations, E_S is the elastic modulus of steel, E_C' is the effective elastic modulus of concrete (considering the creep effect), and ν_C is the Poisson's ratio of concrete. Substitution of Eq 4a into 4b enables the ratio $\varepsilon_{st}(t)/\varepsilon_{SH}(t)$ to be determined as:

$$\frac{\varepsilon_{st}(t)}{\varepsilon_{SH}(t)} = \frac{E'_C}{E_S}\frac{2}{1-\left(\frac{R_{IS}}{R_{OS}}\right)^2}\frac{1}{\frac{E'_C}{E_S}\frac{\left[(1+\nu_S)\left(\frac{R_{IS}}{R_{OS}}\right)^2+(1-\nu_S)\right]}{1-\left(\frac{R_{IS}}{R_{OS}}\right)^2}-\frac{\left[(1+\nu_C)\left(\frac{R_{OC}}{R_{OS}}\right)^2+(1-\nu_C)\right]}{1-\left(\frac{R_{OC}}{R_{OS}}\right)^2}} \tag{5}$$

Equation 5 can now be substituted into Eq 3, which results in an expression for the degree of restraint as only a function of the geometry and material properties (namely, the stiffness and the Poisson's ratio) of concrete and steel:

$$\psi = 1-\frac{E'_C}{E_S}\frac{1}{\frac{E'_C}{E_S}-\frac{1-\left(\frac{R_{IS}}{R_{OS}}\right)^2}{1-\left(\frac{R_{OC}}{R_{OS}}\right)^2}\frac{\left[(1+\nu_C)\left(\frac{R_{OC}}{R_{OS}}\right)^2+(1-\nu_C)\right]}{\left[(1+\nu_S)\left(\frac{R_{IS}}{R_{OS}}\right)^2+(1-\nu_S)\right]}} \tag{6}$$

This enables one to determine the degree of restraint prior to conducting the experiment and provides the opportunity to adjust the test geometry to satisfy the desired degree of restraint that best approximates the actual field conditions.

In addition to determining the degree of restraint, an important parameter that needs to be considered is the magnitude of the strain that will be measured from the inner surface of the steel ring ($\varepsilon_{st}(t)$). From a practical point of view resolving the magnitude of the residual stress in a typical concrete with an accuracy of better than 10 psi (68.9 kPa) requires a minimum steel strain value of 50 $\mu\varepsilon$ before the specimen fails. This can be ensured by determining the minimum value of $\varepsilon_{st}/\varepsilon_{SH}$ at failure for a given ultimate free shrinkage of concrete (ε_{SH}). For example, for a concrete with an ultimate free shrinkage of ε_{SH}=400 $\mu\varepsilon$, a minimum value of at least $\varepsilon_{st}/\varepsilon_{SH}$=0.125 would be desired to obtain a strain in the steel of 50 $\mu\varepsilon$ (ε_{st}=50 $\mu\varepsilon$). Equation 5 can be used to check whether the test geometry satisfies this requirement.

It is now possible to evaluate the effect of specimen geometry on the degree of restraint (Ψ) and $\varepsilon_{st}/\varepsilon_{SH}$. Figure 3(*a*) illustrates the influence of steel ring thicknesses by varying R_{IS}/R_{OS} between 0 (a solid cylinder) and 1 (an infinitely thin ring). As expected, the degree of restraint decreases with decreasing the thickness of steel ring. In addition, a stiffer concrete (higher effective elastic modulus) results in a lower degree of restraint. It is shown that in all cases when R_{IS}/R_{OS} decreases below 0.6, only a slight increase (less than 10 %) in the degree of restraint occurs by further increasing the steel ring thickness. Similarly, Fig. 3(*b*) shows how an increase in the concrete ring thickness (R_{OC}/R_{IC}) reduces the degree of restraint.

Equations 5 and 6 provide an analytical approach to determine the degree of restraint and to ensure that accurate strain measurement can be obtained from the steel ring so that the stress computation can be performed. To illustrate the applicability of this technique for predicting the degree of restraint prior to testing, the degree of restraint determined using Eq 6 was compared with experimentally measured values (using Eq 3), as illustrated in Fig. 4. The experimental data used here was obtained from a series of mortar ring tests with a w/c of 0.30 and 50 % fine aggregate by volume [6]. Three different restrained rings were used with varying the steel thickness (3.2, 9.4, and 19 mm). The geometry parameters were as follows; R_{OC}=225 mm, R_{IC}=R_{OS}=150 mm. The mortar rings were exposed to drying from the top and bottom in a 50 % relative humidity environment. The age dependent effective elastic modulus of concrete was estimated to be 60 % of the actual measured elastic modulus at that age to account for creep effects [24]. The free shrinkage strain ($\varepsilon_{SH}(t)$) and the steel ring strain ($\varepsilon_{st}(t)$) were measured experimentally and used in Eq 3 to calculate the degree of restraint and these results were compared with the values obtained from the analytical solution (Eq 6). It must be noted that the analytical approach discussed earlier is initially developed for a uniform shrinkage condition. However, the results of a series of finite element simulations (as described in the next section) suggest that the analytical approach can be used regardless of the drying condition of the concrete ring. Figure 4 shows that there is reasonable agreement between the analytical approach and the experimentally measured degree of restraint. It is also evident that the degree of restraint decreases over time as the stiffness of concrete increases.

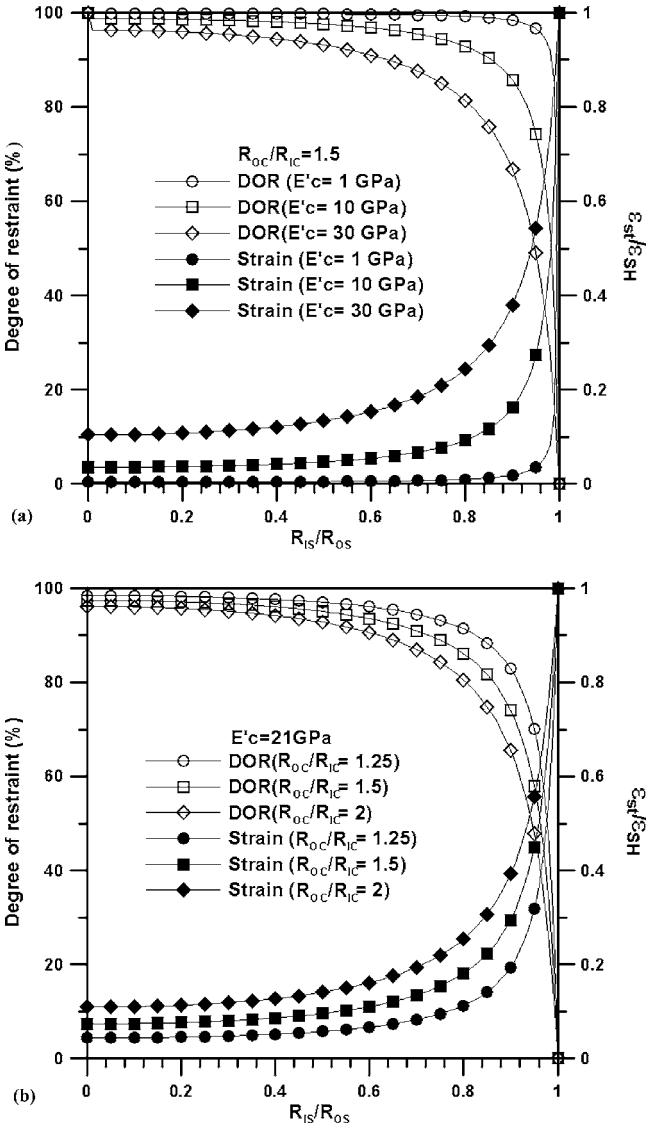

FIG. 3—*The influence of specimen geometry on the degree of restraint and the ratio* $\varepsilon_{st}/\varepsilon_{SH}$*; (a) influence of the concrete stiffness, and (b) influence of the concrete ring thickness* (E'_C=*21 GPa,* E_S=*200 GPa, uniform shrinkage).*

Quantifying the Degree of Restraint in the Presence of Moisture Gradient

To consider how the degree of restraint is influenced by the presence of a moisture gradient inside concrete (caused by preferential drying from exposed surfaces), a series of finite element simulations were performed using the commercial analysis code ANSYS. The ring specimen was considered to be axisymmetric and was modeled using quadrilateral eight node elements. Both rings (concrete and steel rings) were considered to have a height of 75 mm. A fixed value of $R_{IC}=R_{OS}=150$ mm was used in the simulations. In addition, a base value of $R_{OC}=225$ mm and $R_{IS}=140.5$ mm were used; however, for geometrical analysis, the values of R_{OC} and R_{IS} were varied to provide an R_{IS}/R_{OS} ranging from 0.5 to 1 and an R_{OC}/R_{IC} ranging from 1.25 to 2. Other parameters used in the simulations were: $E'_C=21$ GPa, $E_S=200$ GPa, $\nu_c=0.18$, and $\nu_s=0.30$. No creep nonlinearity or microcracking effect was considered in the finite element analysis. A perfectly unbonded condition between the steel and concrete rings was assumed (i.e., no transfer of tensile and shear stresses at the interface). This interface condition can be approached experimentally by using a form release agent or a thin plastic sheet between the concrete and steel [20].

Three different cases of drying were considered: (a) uniform drying, (b) top and bottom drying, and (c) circumferential drying. In cases (b) and (c), a moisture gradient develops inside concrete as it dries preferentially from exposed surfaces. To incorporate moisture gradients in the model, a linear moisture

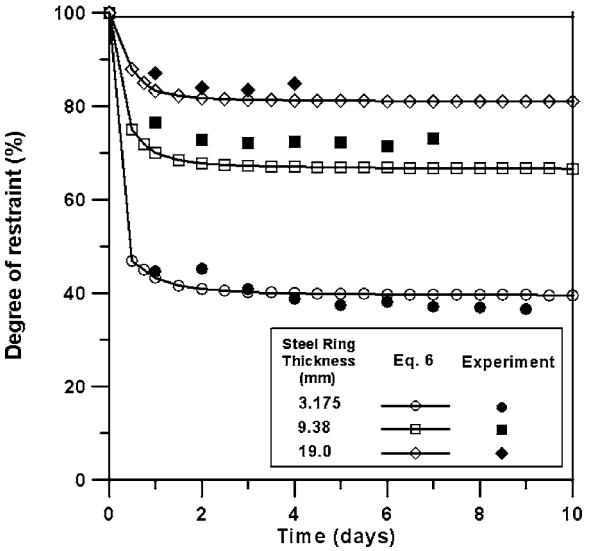

FIG. 4—*Comparison between the analytical solution and the experimentally determined degree of restraint (top and bottom drying).*

diffusion function was used to describe the relative humidity at each point inside concrete as a function of drying time (t), as described by Eq 7 [19].

$$RH(x,t) = RH_I - (RH_I - RH_S)\left[\operatorname{erfc}\left(\frac{x}{2\sqrt{Dt}}\right)\right] \tag{7}$$

where, $RH(x,t)$ is the relative humidity at a depth x from the drying surface, erfc is the complementary error function, RH_S is the relative humidity at the surface of the specimen (considered to be 50 % in the simulations), RH_I is the internal humidity if the specimen was completely sealed (in this paper RH_I was assumed to be 100 % and as such, the effect of autogenous shrinkage was neglected), and D is the aging moisture diffusion coefficient of concrete (m^2/s). It should be noted that although nonlinear diffusion coefficients are commonly suggested for use in concrete [25], and while these equations may be more accurate, the application of a linear coefficient here has enormous computational benefits with no loss in the generalities of the conclusions of this paper. By considering D to be only dependent on specimen age, a single parameter γ can be introduced as $\gamma = 2\sqrt{Dt}$ to represent the time and diffusion coefficient variations in Eq 7. It has been shown that this approach can be used to reasonably describe the moisture gradient that develops inside mortar due to drying [19]. Figure 5 shows an example of relative humidity profiles that correspond to different values of γ. A low γ value (i.e., $\gamma < 0.01$) refers to a very steep moisture gradient, while the severity of the gradient decreases as γ increases. As γ approaches infinity

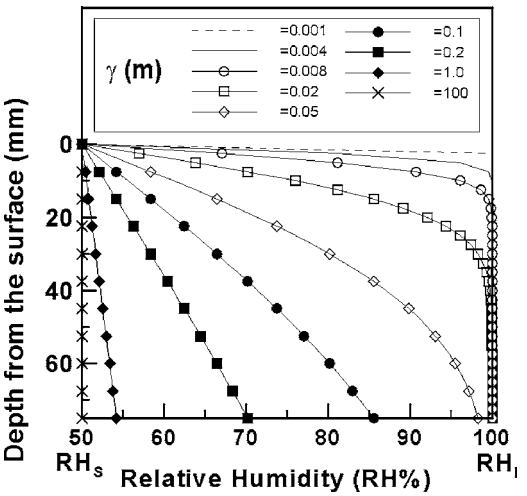

FIG. 5—*The simulated humidity profiles corresponding to different γ values.*

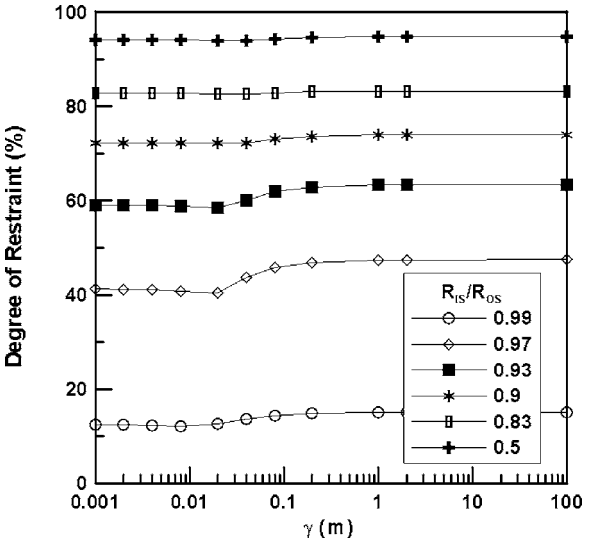

FIG. 6—*Degree of restraint as drying progresses; obtained from finite element simulations (top and bottom drying).*

(practically this corresponds to a $\gamma=100$), the entire cross section of concrete comes to equilibrium with the ambient humidity.

The free shrinkage strain (ε_{SH}) at each point inside concrete can be obtained from the relative humidity using the approach similar to that suggested by [24]. The relationship between shrinkage and relative humidity can be assumed to be linear for high relative humidities (i.e., $RH>50$ %) [18]. In this case, the free shrinkage strain can be estimated as:

$$\varepsilon_{SH}(t)=\varepsilon_{SH-\infty}\frac{100\ \%-RH(x,t)}{100\ \%-RH_S} \tag{8}$$

where $\varepsilon_{SH-\infty}$ is the ultimate free shrinkage of the concrete at a specific ambient relative humidity, RH_S. For the simulations in this paper, a value of $\varepsilon_{SH-\infty}=-100\ \mu\varepsilon$ was assumed at a $RH_S=50$ %; however, the simulation results can be simply scaled to consider other shrinkage values.

The degree of restraint was determined using Eq 1c with values of $U_{SH|R_{IC}}$ and $U_{S|R_{OS}}$ that were determined at the midheight of the ring from the finite element simulations. It was observed that in the case of uniform shrinkage the simulation results match very well with the analytical procedure (Eq 6). For the cases in which a moisture gradient develops inside the concrete (i.e., nonuniform drying), the degree of restraint was determined for different values of the drying time parameter, γ. Figure 6 shows the results for the case of top and bottom drying. It can be seen that a small variation in the degree of restraint occurs as drying progresses. These variations are less than 7 % over the entire duration of drying. Similar results were obtained for concrete experiencing circumferential drying. These results indicate that the degree of restraint is (to a reasonable extent) independent of the moisture profile inside the concrete and as such, the analytical procedure developed for a uniform shrinkage condition (Eq 6) can be employed for other cases of drying to estimate the degree of restraint.

The small variation in the degree of restraint in the cases of nonuniform drying is primarily caused by a nonuniform deformation of the steel ring throughout the height. Figure 7 provides a conceptual illustration of the deformations of the steel ring and the pressure gradient that develops at the concrete-steel interface. When the concrete shrinks uniformly, the interfacial pressure is (almost) uniform across the height (Fig. 7(*a*)). However, in the cases of nonuniform drying, a pressure gradient is observed along the height due to the nonuniform shrinkage inside concrete (Figs. 7(*b*) and 7(*c*)).

To further investigate this behavior, the interfacial pressure gradient was obtained using finite element simulations for a concrete ring experiencing top and bottom drying. The geometrical parameters considered in this case were as follows: $R_{OS}=R_{IC}=150$ mm, $R_{OC}=225$ mm, steel ring thickness=9.38 mm, and height=75 mm. Figure 8(*a*) shows the simulation results in terms of pressure profiles as drying progresses. A higher pressure is always observed in the middle region of the steel ring. Initially, the pressure at the top and bottom regions is zero, which suggests that the top and bottom concrete is not in contact with steel

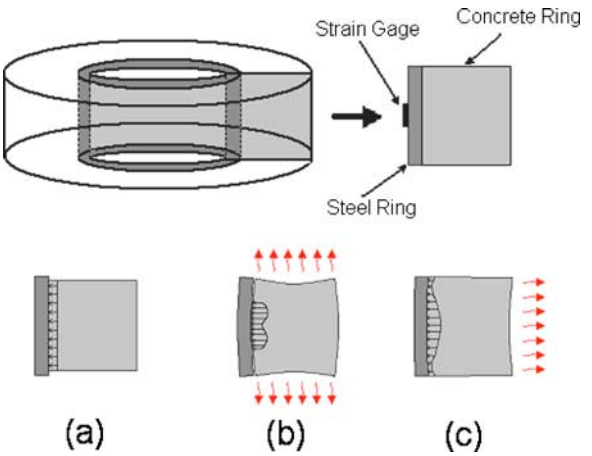

FIG. 7—*Influence of shrinkage condition on the deformation of concrete and steel rings: (a) uniform shrinkage, (b) top and bottom drying, and (c) circumferential drying.*

during this period. However, the pressure increases as drying progresses (i.e., increasing γ) and approaches a more uniform distribution at higher values of γ. The pressure gradient causes a nonuniform strain profile at the inner surface of the steel ring (Fig. 8(*b*)). Due to stress redistribution within the thickness of the steel, the strain profile does not exhibit a significant gradient across the height and as such, has a minor effect on the degree of restraint. Further investigation is required to study the effect of bending for thin and tall steel rings for which bending is expected to be more significant.

Finally, Fig. 9 provides a comparison on the degree of restraint calculated from the analytical procedure (Eq 6, uniform drying) and the results obtained from finite element simulations for the cases of nonuniform drying. The results provided here correspond to a ring with $R_{IC}=R_{OS}=150$ mm, $R_{OC}=225$ mm, height=75 mm, $E'_C=21$ GPa, and $E_s=200$ GPa. The simulations were performed with different values of γ ranging from 0.001 to 100 to determine the degree of restraint as the drying progresses. A good agreement is exhibited between the results obtained from the analytical procedure and the finite element simulations, suggesting that the analytical procedure is capable of estimating the degree of restraint regardless of the direction and uniformity of drying.

A Practical Example of Geometry Selection for the Restrained Ring Test

To illustrate the usefulness of the approach described in this paper, an example is provided in which the geometry of a restrained ring is determined to correspond with an actual field application and to enable reasonable stress measurement. In this example, it is assumed that the field concrete is a floor slab that is 6 in. (152.4 mm) thick and the slab experiences drying from top and bottom surfaces. The concrete has an ultimate free shrinkage of approximately 400 $\mu\varepsilon$ at 50 % relative humidity (i.e., the shrinkage measured using ASTM C 157-04). The actual elastic modulus is assumed to be 25 GPa; however, the effective elastic modulus can be reduced to 15 GPa (60 %) to account for creep effect. Further, the restraint that is observed in a typical floor slab can be calculated to be approximately on the order of 60 %.

A reasonable restrained ring test geometry could consist of a concrete ring that is 6 in. tall and is allowed to dry from the top and bottom surfaces to ensure similar moisture gradients and shrinkage rates as those in the floor. In addition, a concrete ring with circumferential drying could be used, in which case the concrete ring thickness should be 3 in. (i.e., half of the depth as drying occurs from only one side). In this example, the ring with top and bottom drying is considered (however, the same procedure can be applied to determine the desired geometry of the ring with circumferential drying).

From the analytical procedure described earlier (Eqs. 5 and 6), a reasonable target ring geometry can be determined to approximate the condition in the floor. Figure 10 is a graphical representation of Eqs. 5 and 6 and can be used to illustrate different combinations of geometry parameters that satisfy a desired degree of restraint while meeting a minimum value of the ratio $\varepsilon_{st}/\varepsilon_{SH}$ to ensure proper stress calculations. To obtain a ring geometry, first the thickness of the concrete ring should be determined by considering the maximum size of aggregates. In this case, if a 25-mm aggregate is used, the concrete ring thickness can be

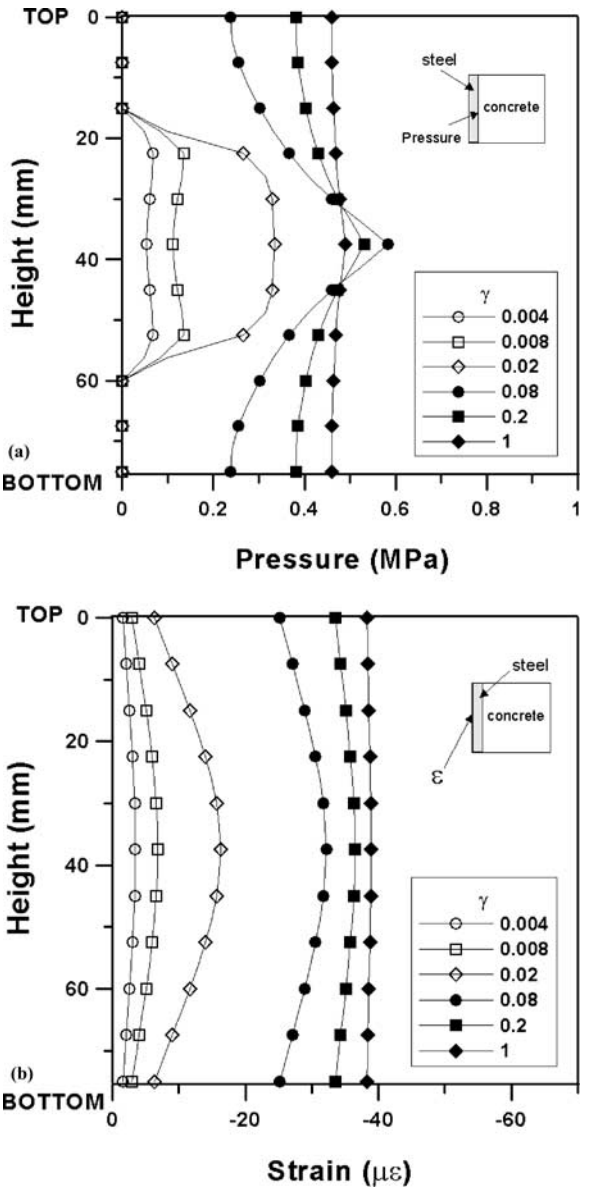

FIG. 8—*The effect of nonuniform deformation of the steel ring (simulations results); (a) pressure gradients at R_{OS}, and (b) steel ring strain at R_{IS}.*

chosen to be 125 mm (5 times the maximum aggregate size). By assuming $R_{IC}=R_{OS}=152.4$ mm (6 in.), the value of R_{OC} will be 277.4 mm. From a practical point of view, a standard 279.4 mm (11 in.) radius cardboard tube form can be used to provide the outer mold for the concrete ring. This gives an $R_{OC}=279.4$ mm, which yields an $R_{OC}/R_{IC}=1.83$. From Fig. 10(*a*), to achieve a 60 % degree of restraint, $R_{IS}/R_{OS}=0.947$ is obtained which gives a steel ring thickness of 8.08 mm. A commercially available steel ring with 9.5 mm (3/8 in.) thickness can be chosen (outer radius is 6 in.). This corresponds to an $R_{IS}/R_{OS}=0.938$ and a degree of restraint of $\psi=63.8\%$ which is quite similar to 60 % and is therefore acceptable for practical purposes (as shown as a solid point in Fig. 10(*a*)).

The next step is to check the value of $\varepsilon_{st}/\varepsilon_{SH}$ to ensure proper stress calculations. Using the ultimate free shrinkage of concrete ($\varepsilon_{SH}=400\ \mu\varepsilon$), a minimum acceptable value of $\varepsilon_{st}/\varepsilon_{SH}=50/400=0.125$ is desired. From Fig. 10(*b*), the solid point corresponding to $R_{OC}/R_{IC}=1.83$ and $R_{IS}/R_{OS}=0.947$ lies above the $\varepsilon_{st}/\varepsilon_{SH}=0.125$ curve, and as such, the strain ratio requirement is also satisfied.

Finally, the actual maximum residual stress that develops inside the concrete ring can be calculated using the method suggested by Hossain and Weiss [6]; Eq 9:

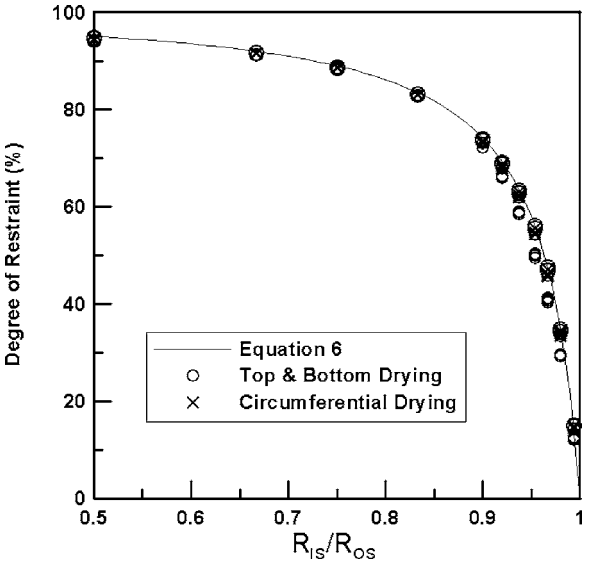

FIG. 9—*Comparison on the degree of restraint obtained from the analytical procedure (Eq 6, uniform drying) and the values obtained from finite element simulations (nonuniform drying).*

$$\sigma_{Actual-max} = -\varepsilon_{st}(t)E_S\left(\frac{R_{IC}^2 + R_{OC}^2}{R_{OC}^2 - R_{IC}^2}\right)\left(\frac{R_{IC}^2 - R_{IS}^2}{2R_{IC}^2}\right) \tag{9}$$

It should be noted that this equation is applicable only when shrinkage is uniform in the radial direction (i.e., uniform drying or top and bottom drying), and an alternative formula (as described elsewhere [20]) needs to be used for the case of circumferential drying.

To summarize, the final geometry of the restrained ring test can be selected as follows; concrete ring with 279.4 mm (11 in.) outer radius (R_{OC}) and steel ring with 152.4 mm (6 in.) outer radius (R_{OS}) and 9.5 mm (3/8 in.) thickness. Both rings are 6 in. high. A standard 279.4 mm (11 in.) radius cardboard tube form is used as the outer mold for the concrete ring.

Summary and Conclusions

Based on the results presented in this paper, the following conclusions can be drawn:

- To utilize the restrained ring test method to simulate an actual field condition requires that an appropriate specimen geometry be determined prior to performing the experiment. The geometry of the ring test that should be selected for a particular application must satisfy a desired degree of restraint, match the actual drying conditions in the field, and ensure proper strain measurements to enable accurate stress calculations.
- An analytical procedure was presented to determine the degree of restraint in the restrained ring test for concrete under uniform shrinkage (Eq 6). It was shown that the degree of restraint depends only on the geometry of the rings and the material properties (namely the elastic modulus and the Poisson's ratio) of the concrete and the steel. The degree of restraint increases with increasing the thickness and elastic modulus of the restraining ring (steel) and decreases with increasing the thickness of the concrete ring. In addition, it was shown that to ensure proper stress calculations inside the concrete ring, a minimum acceptable strain ratio $\varepsilon_{st}/\varepsilon_{SH}$ must be met. This imposes an additional requirement on the restrained ring geometry (Eq 5).
- A series of finite element simulations were performed to examine the applicability of the analytical solution to the cases of nonuniform (i.e., top and bottom or circumferential) drying in which a moisture gradient develops inside the concrete ring. It was observed that the degree of restraint shows minor changes as the drying progresses and is not significantly influenced by the presence of a moisture gradient inside the concrete ring. This suggests that the analytical solution that was initially developed for uniform shrinkage is also applicable to estimate the degree of restraint in the cases of nonuniform drying. It should, however, be noted that drying direction can significantly

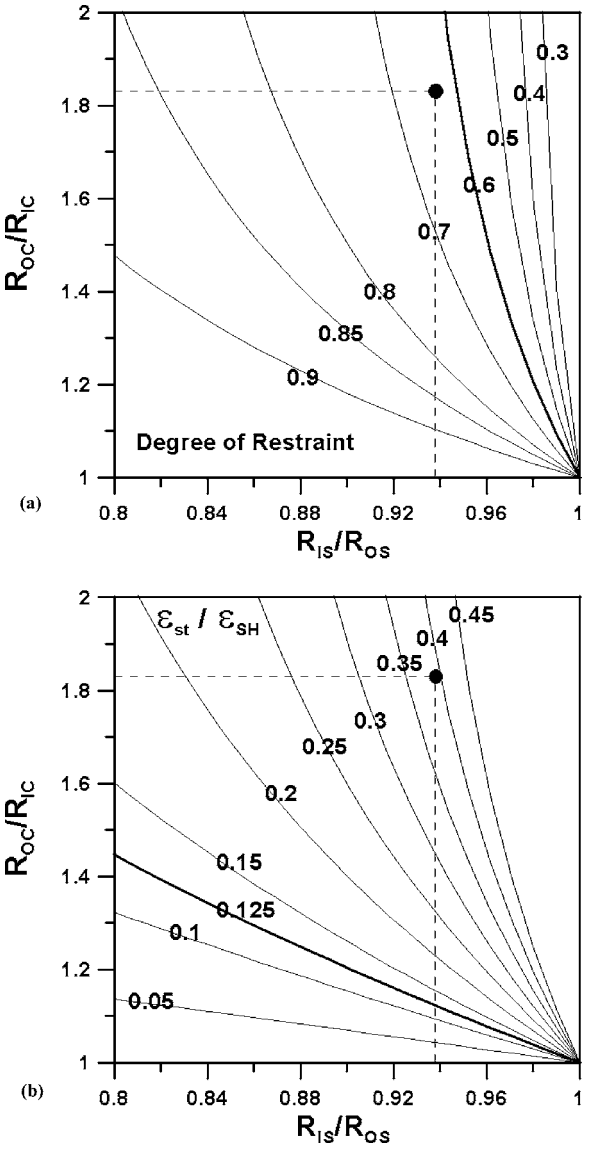

FIG. 10—*Graphical representation of Eqs. 5 and 6 in terms of possible combinations of geometry parameters for a desired degree of restraint (a) and an acceptable strain ratio (b) (assumed material properties:* E'_C*=15 GPa,* E_S*=200 GPa,* ν_C*=0.18, and* ν_S*=0.3).*

influence the distribution of residual stresses inside the concrete ring [20] and must not be neglected during stress calculations.

Acknowledgments

The authors gratefully acknowledge partial support for this work that was received from the National Science Foundation under Grant No. 0134272: a CAREER AWARD granted to the fourth author. Any opinions, findings and conclusions or recommendations expressed in this material are those of the author(s) and do not necessarily reflect the views of the National Science Foundation (NSF). This work was conducted in the Concrete Materials and Sensing Laboratories at Purdue University, as such the authors gratefully acknowledge the support that makes this possible.

References

[1] Weiss, W. J., Yang, W., and Shah, S. P., "Influence of Specimen Size and Geometry on Shrinkage Cracking," *J. Eng. Mech.*, Vol. 126, No. 1, 2000, pp. 93–101.

[2] Swamy, R. N. and Stavrides, H., "Influence of Fiber Reinforcement on Restrained Shrinkage Cracking," *ACI J.*, Vol. 76, No. 3, 1979, pp. 443–460.
[3] Carlson, R. W. and Reading, T. J., "Model of Studying Shrinkage Cracking in Concrete Building Walls," *ACI Struct. J.*, Vol. 85, No. 4, 1988, pp. 395–404.
[4] Wiegrink, K., Marinkunte, S., and Shah, S. P., "Shrinkage Cracking of High Strength," *ACI Mater. J.*, Vol. 93, No. 5, 1996, pp. 409–415.
[5] Grzybowski, M. and Shah, S. P., "Shrinkage Cracking of Fiber Reinforced Concrete," *ACI Mater. J.*, Vol. 87, No. 2, March/April 1990, pp. 138–148.
[6] Hossain, A. B. and Weiss, W. J., "Assessing Residual Stress Development and Stress Relaxation in Restrained Concrete Ring Specimens," *Cem. Concr. Compos.*, Vol. 26, 2004, pp. 531–540.
[7] Springenschmidt, R., Gierlinger, E., and Kernozycki, W., "Thermal Stress in Mass Concrete: A New Testing Method and the Influence of Different Cements," *Proceedings of the 15th International Congress for Large Dams*, Lausanne, 1985, R4, pp. 57–72.
[8] Weiss, W. J., Yang, W., and Shah, S. P., "Shrinkage Cracking of Restrained Concrete Slabs," *J. Eng. Mech.*, Vol. 124, No. 7, 1998, pp. 765–774.
[9] Kovler, K., "Testing System for Determining the Mechanical Behavior of Early Age Concrete Under Restrained and Free Uniaxial Shrinkage," *Mater. Struct.*, London, U.K., Vol. 27, No. 170, 1994, pp. 324–330.
[10] Toma, G., Pigeon, M., Marchand, J., and Bercelo, L., "Early-Age Autogenous Restrained Shrinkage: Stress Build Up and Relaxation," *Self-Desiccation and Its Importance in Concrete Technology*, B. Persson, and G. Fagerlund, Eds., Lund Institute of Technology, Lund, Sweden, 1999, pp. 61–72.
[11] Altoubat, S. A. and Lange, D., "Grip-Specimen Interaction in Uniaxial Restained Test," ACI-SP 206, *Concrete: Material Science to Application: A Tribute To Surendra P. Shah*, American Concrete Institute, Farmington Hills, MI, 2002, pp. 189–204.
[12] Weiss, W. J., "Prediction of Early-Age Shrinkage Cracking in Concrete," Ph.D. Thesis, Northwestern University, Evanston, Illinois, 1999.
[13] Kovler, K., Sikuler, J., and Bentur, A., "Restrained Shrinkage Tests of Fiber Reinforced Concrete Ring Specimens: Effect of Core Thermal Expansion," *ACI Mater. J.*, Vol. 26, 1993, pp. 231–237.
[14] Attiogbe, E. K., Weiss, W. J., and See, H. T., "A Look at the Stress Rate Versus Time of Cracking Relationship Observed in The Restrained Ring Test," *The Advances in Concrete Through Science and Engineering, a Rilem International Conference*, Northwestern University, Evanston, IL, March 2004 (Electronic proceedings).
[15] Attiogbe, E. K., See, H. T., and Miltenberger, M. A., "Cracking Potential of Concrete Under Restrained Shrinkage," *Proceedings, Advances in Cement and Concrete: Volume Changes, Cracking, and Durability*, Engineering Conferences International, Copper Mountain, Colorado, August 10–14, 2003, pp. 191–200.
[16] NCHRP Report 380, "Transverse Cracking in Newly Constructed Bridge Decks," National Cooperative Highway Research Program, National Academy Press, Washington, DC, 1995.
[17] Hossain, A. B. and Weiss, W. J., "The Role of Specimen Geometry and Boundary Conditions on Stress Development and Cracking in the Restrained Ring Test," *Cement and Concrete Research*, Vol. 36, No. 1, 2006, pp. 189–199.
[18] Weiss, W. J. and Shah, S. P., "Restrained Shrinkage Cracking: The Role of Shrinkage Reducing Admixtures and Specimen Geometry," *RILEM International Conference on Early-Age Cracking in Cementitious Systems (EAC'01)*, K. Kovler and A. Bentur, Eds., Haifa Israel, 2001, pp. 145–158.
[19] Moon, J. H., Rajabipour, F., and Weiss, W. J., "Incorporating Moisture Diffusion in the Analysis of the Restrained Ring Test," *Proceedings of the Fourth International Conference on Concrete under Severe Conditions (Environment & Loading), Seoul National University & Korea Concrete Institute*, Seoul, Korea, June, 2004, pp. 1973–1980.
[20] Moon, J. H. and Weiss, W. J., "Estimating Residual Stress in the Restrained Ring Test under Circumferential Drying," *Cement and Concrete Composites*, Vol. 28, No. 5, 2006, pp. 486–496.
[21] See, H. T., Attiogbe, E. K., and Miltenberger, M. A., "Shrinkage Cracking Characteristics of Concrete Using Ring Specimens," *ACI Mater. J.*, Vol. 100, No. 3, May/June 2003, pp. 239–245.
[22] ACI's Manual of Concrete Practice; 207.2R, "Effect of Restraint, Volume Change, and Reinforcement on Cracking of Mass Concrete," American Concrete Institute, Farmington Hills, MI, 1995.

[23] Hossain, A. B., Pease, B. J., and Weiss, W. J., "Quantifying Early-Age Stress Development and Cracking in Low w/c Concrete Using the Restrained Ring Test with Acoustic Emission," *Transportation Research Record, Concrete Materials and Construction 1834*, Transportation Research Board, Washington, DC, pp. 24–33.

[24] Bazant, Z. P. and Wittmann, F. H., *Creep and Shrinkage in Concrete Structures*, John Wiley & Sons, New York, 1982, pp. 163–256.

[25] Bazant, Z. P. and Najjar, L. J., "Drying of Concrete as a Nonlinear Diffusion Problem," *Cem. Concr. Res.*, Vol. 1, 1971, pp. 461–473.